PERFORMANCE OF RF SYSTEM FOR COMPACT-ERL MAIN LINAC AT KEK

T. Miura[#] , M. Akemoto, D. Arakawa, H. Katagiri, T. Shidara, T. Takenaka, K. Nakao, H. Nakajima, S. Fukuda, H. Honma, H. Matsushita, T. Matsumoto, S. Michizono, Y. Yano, F. Qiu, A. Akiyama, H. Sakai, K. Umemori, KEK, Tsukuba, 305-0801, Japan

Abstract

The construction of the compact Energy Recovery LINAC (cERL) in KEK was completed at the end of 2013, and the beam commissioning has begun. Solid-state amplifiers were employed as the RF power sources in the main LINAC (ML). Cavity field feedback and tuner feedback control were performed using the digital low-level RF (LLRF) system. Large microphonics was observed, but the effect was suppressed well by the digital LLRF system.

INTRODUCTION

The compact Energy Recovery LINAC (cERL) is the test facility for the 3 GeV ERL planned as the future light source at KEK. As shown in Fig. 1, the cERL consists of the photocathode DC gun, injector LINAC, main LINAC (ML), and return loop. A normal-conducting buncher cavity and three two-cell superconducting (SC) cavities were installed in the injector. Two nine-cell SC cavities were installed in the ML. The injected beam is accelerated in the ML, and the beam is decelerated at the ML down to the injection energy after circulating through the return loop and then dumped. For a low-emittance beam, a highly stable cavity field is required. The requirements for the 3 GeV ERL are 0.01%rms in amplitude and 0.01° rms in phase. The requirements for the RF stability of the cERL are less than 0.1% rms in amplitude and 0.1° rms in phase.
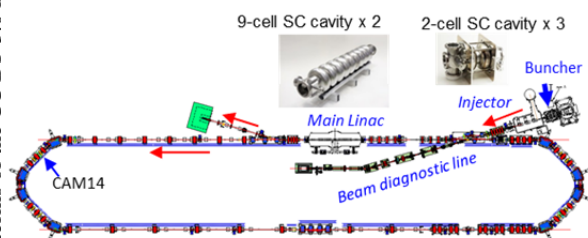

Figure 1: Plan view of cERL.

The construction of the injector was completed in April 2013 and the beam commissioning in the injector has begun. The RF was stabilized using a digital feedback system. We already reported the RF commissioning results of the injector [1].

The construction of the entire cERL was completed by the end of 2013, and beam commissioning has begun. As a result of commissioning, the accelerated beam was

successfully transported the return loop, and the beam was dumped after deceleration in the ML [2]. This paper reports mainly the RF commissioning and performance of the ML.

HIGH LEVEL RF SYSTEM

The ML has two nine-cell SC cavities, MLSC1 and MLSC2. The RF frequency of the cERL is 1.3 GHz. The loaded quality factors (Q_L) of MLSC1 and MLSC2 are 1.3×10^7 and 1.0×10^7, respectively. In the ML, the energy of the beam acceleration is recovered by deceleration; thus, the beam loading can be small. On the other hand, the large detuning caused by microphonics was a concern before operation. The cavity unit testing revealed that a large power source is not necessary. Therefore, a 16 kW solid-state amplifier (SSA) and 8 kW SSA were employed as high power RF sources for MLSC1 and MLSC2, respectively, as shown in Fig. 2. The SSA is compact, stable, and reliable.

Figure 2: RF power sources in ML: 16 kW (right) and 8 kW (left) SSAs.

LOW LEVEL RF SYSTEM

For RF feedback control, the digital low-level RF (LLRF) system using micro-TCA digital boards [3] is used in cERL, as shown in Fig. 3. The boards consist of a base card and two daughter cards, an analog-to-digital conversion (ADC) card and a digital-to-analog conversion (DAC) card, as shown in Fig. 3. The field-programmable gate array (FPGA: Vertex5FXT), the digital I/O, and an external trigger port are on the base card. The ADC card is equipped with four 16-bit ADCs (LTC2208) and a clock input. The DAC card is equipped with two dual DACs (AD9783). Embedded Linux is installed in a PowerPC on the FPGA. The experimental physics and industrial control system (EPICS) is installed

for communication control, and each board act as an EPICS IOC. Two boards are used for each cavity, one is for the RF field feedback control and the other is for tuner control.

Figure 3: MicroTCA digital feedback boards.

RF Field Feedback Control

Figure 4 shows a schematic diagram of the digital feedback system. The master oscillator (MO) frequency of the cERL is the same as the RF frequency, 1.3 GHz. The local oscillator frequency is 1310.1565 MHz. The cavity pick-up signal of 1.3 GHz is down-converted to an intermediate frequency (IF) of 10.15625 MHz, which is 1/128 of the MO frequency. The sampling frequency of the ADC is 81.25 MHz, which is 1/16 of the MO frequency. The sampled data are separated into in-phase (I) and quadrature (Q) components. After the phase for the I/Q are corrected using a rotation matrix, the I/Q data pass through the infinite impulse response (IIR) low-pass filter [4], which is important because it rejects the excitation due to parasitic modes, such as an $8/9\pi$ mode in the nine-cell cavity. The feedback is performed by proportional-integral control. The baseband I/Q signals from the DAC card are fed to the IQ modulator. Finally, the amplified 1.3 GHz RF is fed to the cavity. The parameters such as the feedback gain and filter were determined by parameter scanning [4].
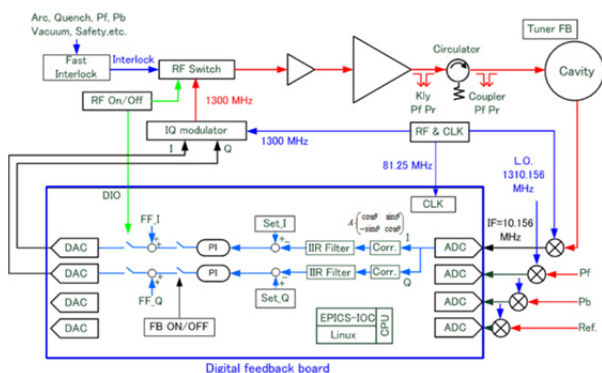

Figure 4: Schematic diagram of digital feedback system.

Tuner Feedback Control

Each cavity has a mechanical tuner and a piezo tuner, which are used for coarse and fine tuning of the cavity resonant frequency, respectively [5]. The tuners are controlled using the same boards as for the RF field feedback. The stepping motor for mechanical tuner and piezo tuner are controlled by using the outputs of the

digital I/O and the DAC output of the FPGA board, respectively.

A tuner control diagram is shown in Fig. 5. The feedback logic in the FPGA is very similar to that of the RF field feedback. The phase is calibrated by setteing the phase difference ($\Delta\theta$) between the cavity input RF (θ_f) and the cavity pickup signal (θ_c) to zero at the resonant point. Figure 6 shows a result of a resonance search in MLSC1 by scanning the DAC-offset. After phase correction, each phase datum passes through the IIR filter as a first-order low-pass filter. The current set value of the cut-off frequency is about 10 Hz. Tuner feedback is performed to maintain $\Delta\theta$ at zero. The amplitude thresholds were established to maintain the reliability of the phase measurement.

As shown in Fig. 5, the feedback method of piezo and mechanical tuners differ. For the piezo tuner, feedback is the only integral control for $\Delta\theta$. The center voltage of piezo is 250V, and the piezo is driven between 0 V and 500 V by the amplified DAC output of the digital board. When interlock occurs, the frequency feedback is turned off, and the piezo value is maintained using the hold value as shown in Fig. 5. Furthermore, to protect the piezo from rapid and large changes, IIR low-pass filter is installed in front of the DAC output. In contrast, for the mechanical tuner feedback, pulses in the clockwise (CW) or counterclockwise (CCW) directions are output in proportion to $\Delta\theta$. For SC cavities, the piezo tuner is sufficient for frequency feedback. On the other hand, frequency feedback of the normal-conducting buncher cavity is performed by only for the mechanical tuner.
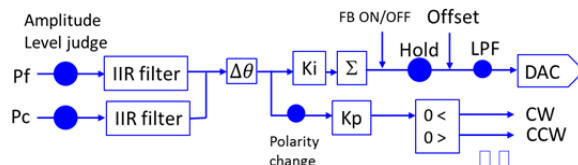

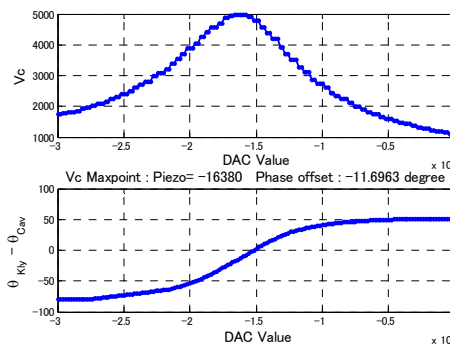Figure 5: Schematic diagram of tuner control.

Figure 6: Resonance search by scanning DAC-offset. Phase is calibrated by setting $\Delta\theta$=0 at the maximum point of V_c.

The Q_L values of the ML cavities are around 10^7, so the cavity band width is approximately ±65 Hz. For such

a large Q_L, detuning due to microphonics was a concerned. Figure 7 shows the result of the $\Delta\theta$ feedback for 3 h. $\Delta\theta$ was controlled less than a few degrees by the tuner feedback. This corresponds a few hertz of detuning.
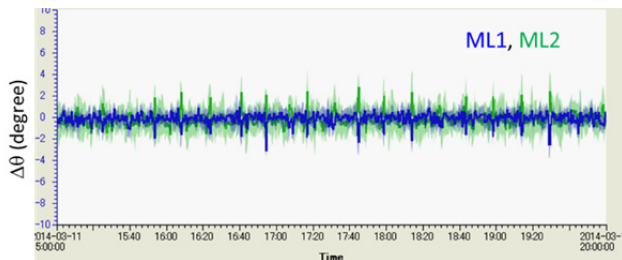

Figure 7: Plot of the detuning angle of the ML cavities.

RF STABILITY

Figure 8 shows waveforms of the input RF (V_f) and cavity pick up (V_c) of MLSC2 during operation without feedback. The stability of the amplitude of V_c does not differ greatly from that of V_f, however, the phase fluctuation of V_c is much greater than that of V_f because of microphonics.
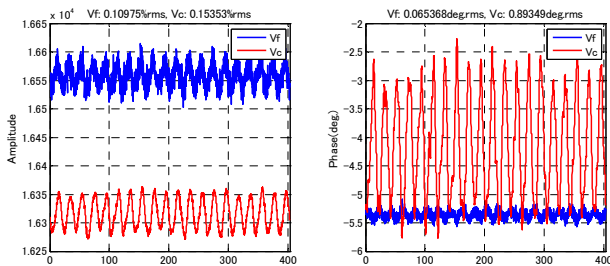

Figure 8: Waveforms of input RF (V_f) and cavity pickup (V_c) of MLSC2 during operation without feedback.

Figure 9 shows a waveform of V_c of MLSC2 during operation with feedback. Stabilities of MLSC1 and MLSC2 with feedback are 0.012% rms and 0.013% rms in amplitude, 0.014° rms and 0.015° rms in phase, respectively. These results satisfy requirement of cERL.
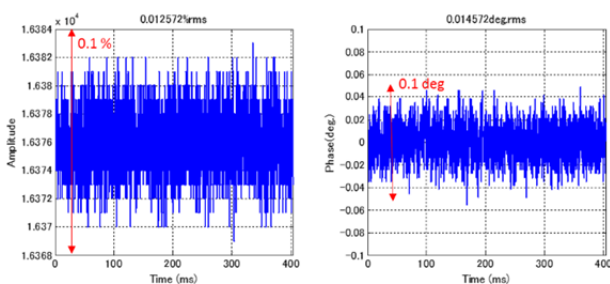

Figure 9: Stability of V_c of MLSC2 with feedback: 0.013% rms in amplitude and 0.015° rms in phase.

The phase noise was also measured with a signal source analyzer. Figure 10 shows the phase noise spectra from 10 Hz to 1 MHz. A large phase noise caused by the microphonics was observed from 10 Hz to around 500 Hz in the both cavities, MLSC1 and MLSC2. During feedback operation, the phase noise due to microphonics was suppressed, and the phase noise of V_c was almost the same as that of the MO. The integral phase jitter from 10Hz to 1 MHz was around 0.017° rms, which is consistent with the result for our digital LLRF system.
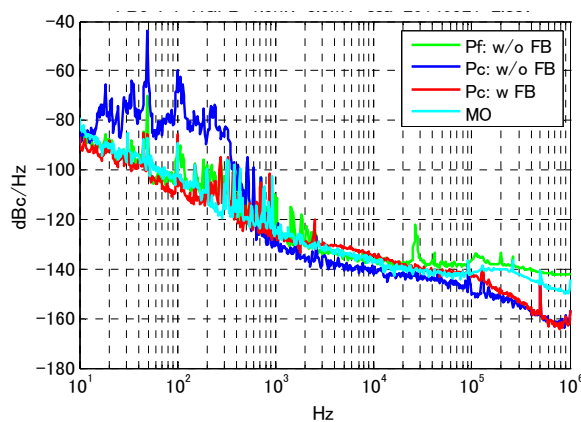

Figure 10: Results of phase noise measurements of MLSC2 using a signal source analyzer; green and blue: input RF and cavity signal w/o feedback, red: cavity signal with feedback, cyan: MO.

SUMMARY

The construction of the cERL has been completed, and commissioning has begun. SSAs were employed as the high-power RF sources of the ML. RF field feedback and tuner feedback were performed by a digital LLRF system using FPGA boards. The effect of microphonics was damped well by the digital feedback system. RF stabilities of MLSC1 and MLSC2 are 0.012%rms and 0.013%rms in amplitude, and 0.014° rms and 0.015° rms in phase, respectively.

REFERENCES

[1] T. Miura et al., "Performance of RF System for Compact ERL Injector in KEK", Proc. of ERL2013, Novosibirsk, WG306.

[2] M. Shimada et al., "Commissioning of a Recirculation Loop of the Compact ERL at KEK", MOPRO111, these proceedings.

[3] T. Miura et al., "Low-Level RF System for cERL", Proc. of IPAC'10, Kyoto, pp.1440-1442 (2010).

[4] F. Qiu et al., "Performance of the Digital LLRF System at cERL", WEPME072, these proceedings.

[5] K. Enami et al., "Performance Evaluation of Compact ERL Main Linac Tunerer", WEPRI027, these proceedings.